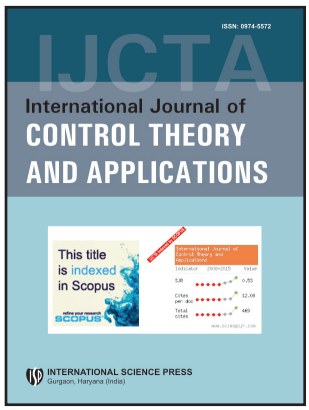


**International Journal of Control Theory and Applications**

ISSN : 0974-5572



**Volume 10 • Number 12 • 2017**

# ACADS: An Automatic Computer Aided Diagnostic System for Oil Spill Detection and Classification in SAR Images

**J. Senthil Murugan[a] and V. Parthasarathy[b]**

[a]*Research scholar, Department of Computer Science and Engineering, St Peter's University, Avadi, Chennai, Tamil Nadu*
[b]*Professor, Computer Science and Engineering, Vel Tech Multi Tech Dr. Rangarajan Dr. Sakunthala Engineering College, Avadi, Chennai, India*

***Abstract:*** The primary goal of this paper is to build up a completely Automatic Computer Aided Diagnostic System (ACADS) for the detection of oil spills in SAR images. In order to do this, the whole proposed ACADS is carried out in four distinct stages: (i). Read and Preprocess the input image, (ii). Binary Operation based Image Segmentation, (iii). Feature Extraction, (iv). And classification of the oil spill portion. Initially, the input image is read from the database or imaging devices that are connected to a PC or given by the user is verified for noise. The noise could be removed by the use of filters. Enhanced Histogram Equalization (EHE) method is used to increase the quality of the image. In the second stage, the binary operations are applied continuously to detect and segment the oil spills that occurs in the enhanced image. In the third stage, the statistical features are extracted from the segmented image and it is classified using Multi-Class SVM classifier in the final stage. This ACADS approach is implemented and verified in MATLAB software from the obtained results. By comparing the ACADS's results with the existing system results, the performance is evaluated.

***Keywords:*** Object Detection, Image Processing, SAR images, Oil Spill Detection, Features Extraction and Classification.

## 1. INTRODUCTION

The Synthetic Aperture Radar (SAR) images can be acquired from satellites such as ERS, JERS and RADARSAT. When interpreting radar images, a special care should be taken since the radar interacts with the ground features in ways different from the optical radiation. An example of an ERS SAR image is shown in Figure 1, together with a SPOT multispectral natural color composite image of the same area for comparison.

The left urban area appears bright in the SAR image while the right vegetated areas have intermediate tone. Also in the image, the clearings and water (sea and river) appear dark. These features will be described in the following sections. The SAR image was obtained in September 1995 while the SPOT image was obtained in February 1994. The additional clearings can be found in the SAR image. The radar images are formed by

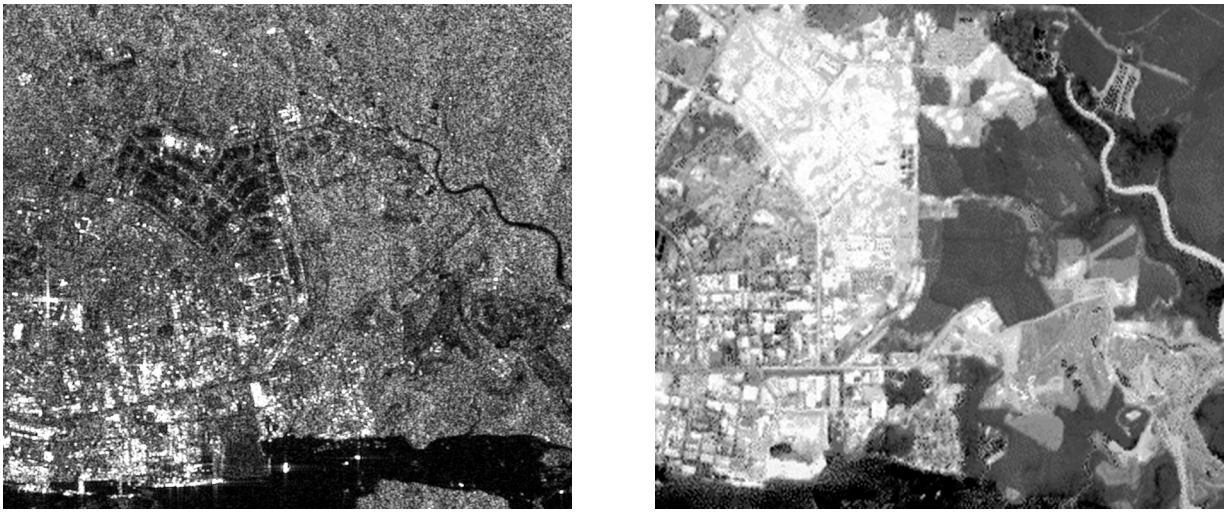

**ERS SAR image (pixel size = 12.5 m)**

**SPOT Multispectral image in Natural Color (pixel size = 20 m)**

**Figure 1: Sample SAR Images**

the coherent interaction of the transmitted microwave with the targets which is different from optical images. Thus, it suffers from the effects of speckle noise which emerges from the coherent summation of the signals scattered from ground scatters, distributed randomly within each pixel. A radar image seems to be noisier than an optical image. Before display and analysis, the speckle removal filter may be applied to the digital image for suppressing the speckle noise.

The high-resolution images from broad areas of terrain are obtained by using the Synthetic Aperture Radar (SAR). SAR has the ability to operate under inclement weather conditions, day or night. The processing of SAR data is desired to extract relevant features, such as objects or buildings. The detection of such objects is based on the detection of locally bright pixels, followed by clustering of neighborhoods of pixels. Remote sensing is valuable in a few methods of oil spill control, including large area surveillance, site specific monitoring and tactical assistance in crises. Remote detecting can provide basic data to upgrade strategic and tactical decision-making, potentially reducing incidence of spills by providing a deterrent factor, decreasing response costs by facilitating rapid oil recovery and ultimately minimizing impact.

Marine oil spills can be isolated into two classifications of significance to the type of remote sensing technology, which may be utilized to identify and react to the incidents. The first category is non-accidental discharges, which can incorporate incidental losses from vessels because of the hull or equipment leaks, as well as the oil discharged deliberately during De-ballasting and tank-cleaning activities. While these non-accidental discharges have a tendency to be little in them, they are frequent and contribute a great deal more to the general acquaintance of oil with the marine environment than accidental spills, and are expanding worldwide administrative concern. Accidental spills typically involves much larger releases of oil though it is less frequent and such oil spills are said to be high profile events for which rapid and effective emergency response is required to contain and recover the spilled oil. In numerous nations, appropriate and effective response capability is required by law, for instance, demanded by the *Oil Pollution Act* of 1990 in the USA, as well as by recent amendments to the *Canada Shipping Act* in Canada. There is a growing recognition that using remote sensing, especially airborne, to assist cleanup response efforts could mitigate the impacts of oil on the environment, as well as reduce cleanup costs.

But, in this paper the contribution of the paper is: Read the SAR image as input image, Preprocess the image by noise removal and enhance the image using histogram equalization, Oil spill detection using

morphological operations, feature extraction using GLCM method and classify the features using Mulit-Class SVM classifier.

## 2. BACKGROUND STUDY

Oil spills on the ocean surface are seen frequently. The observed oil spills correlate well with the major shipping routes (e.g. In the Southeast Asian Waters (Lu, 2003; Lu et. al., 1999), and in the Yellow and East China Sea (Ivanov et. al., 2002) and commonly appear in connection with offshore installations (e.g. In the North Sea (Espedal & Johannessen, 2000). The oil contamination in the seas per annum is of 48% fuels and 29% crude oil. Only 5% of all pollution entering into the ocean (Fingas, 2001) is contributed by the tanker accidents.

The European Space Agency (1998) indicated that 45% of the oil pollution originates from the operative discharges from ships. At the point when considering how incessant such spillages happen, controlled normal oil spills can be a much greater threat to the marine environment and the biological system than larger oil spill accidents like the Prestige tanker (conveying N77,000 tons of fuel oil (Oceanides Web-webpage, 2004)accidentat Galice, northwest coast of Spain in 2002. The effect of not checking oil spills is presently unknown, but the main environmental impact is assumed to be seabirds erroneously landing on them and the damage to the coastal ecology as spills hit the beach (Shepherd, 2004). Simecek-Beatty and Clemente-Colon (2004) portrays how oiledbirds prompt to the utilization of SAR for locating a sunken vessel leaking oil.

The another passive sensor is MWR. The instrument takes a glance at the microwave radiation in the wavelength cm to mm range that the ocean emanates, and has consequently been weather independent (Trieschmann et. al., 2003). Oil spills transmit more grounded microwave radiation than the water and appear as bright objects on a darker ocean. As indicated by Robinson (1994), oil spills can have solid surface-emissivity signatures, however, as a spatial resolution of tens to hundreds of meters is attractive for the oil slicks determination. This sort of sensors for oil slick thickness monitoring are most properly sought after via aircraft sensor. Zhifu et. al., (2002) did a few analyses utilizing airborne (AMR-OS) and a ship borne (K-band) MWRs looking at different oil types and thickness. They found that MWRs are useful apparatuses for measuring the thickness and evaluating the volume of the spills, yet the resolution is not sufficiently fine to give precise outcomes. Fingas and Brown (1997) outline the studies done in this field and presume that the capability of radiometers as a dependable gadget for measuring spill thickness is dubious.

The Oil spills can occur amid oil transportation or capacity and spillage can occur in water, ice or ashore. Marine oil spills can be profoundly unsafe since wind, waves and current can disperse a huge oil spill over a wide region within a few hours in the untamed ocean (Fingas, 2001). Somewhere around 1988 and 2000, there were 2,475 spills which discharged more than 800,000 liters of oil in Toronto and its encompassing areas (Li, 2002). An oil spill might be because of various reasons, including transportation accidents. Besides accidents, the controlled release of oil by shipping operators and oil production platforms are major sources of oil spills (Grüner,1991). The oil spills could be prevented by imposing ecological standards, regulations and strict operating procedures, however these measures can't totally take out the hazard (Fingas, 2001).When oil is spilled, it rapidly spreads to form a thin layer on the water surface, known as an "oil slick". Over the long haul, the oil spill gets to be distinctly more slender, forming a layer known as a "sheen" which has a rainbow like appearance. Light oils are highly toxic, yet dissipates rapidly. Heavy oils are less toxic but persist in the environment for a long time. Heavy oils can get blended with rocks and sandy shorelines where they may endure for years (Environment Canada, 2007). Around the world, fuels account for 48% of the aggregate oil spilled into the ocean worldwide, while crude oil spills represent 29% of the aggregate (Brekke and Solberg, 2005).From the above literature survey it is clear and noticed that a squency of image processing steps are applied on SAR images to detect and classify the oil spills occur on the image. The entire functionality of the ACADS is illustrated in Figure 2.

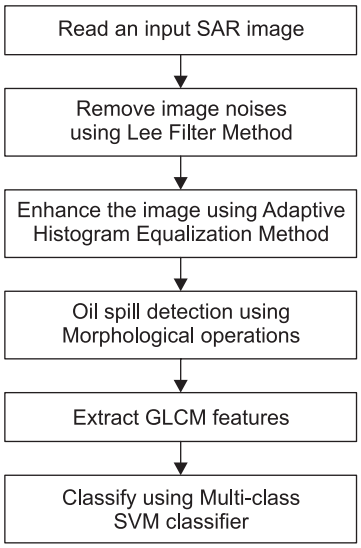


**Figure 2: Overall Functionality of Proposed ACADS**

The entire functionality of the proposed ACADS is illusterated in Figure 2 and each stage of the ACADS is described briefly below.

## 3. NOISE REMOVAL USING LEE FILTER

The Lee filter is a very familiar statistical filter derived from both the additive and multiplicative noise. It is designed to eliminate speckle noise while preserving edges and point features in SAR imagery. A smoothed pixel for the multiplicative noise model based on the Minimum Mean Square Error (MMSE) criterion can be represented as follows:

$$\hat{I}(x, y) = \bar{I}_s + K_s (I_{(x, y)} - \bar{I}_s)$$

where $\bar{I}_s$ is the mean value of the intensity within the filter window $\eta_s$, and $K_s$ is the adaptive filter coefficient determined by

$$K_s = 1 - \frac{C_u^2}{C_s^2}$$

Here,

$$C_s^2 = \frac{(1/\eta_s) \sum_{x, y e\eta} (I_{(x, y)} - \bar{I}_s)^2}{(I_{(x, y)} - \bar{I}_s)^2}$$

and $C_u^2$ is a constant for a given image and can be determined by either

$$C_u^2 = \frac{\text{var}(z')}{(\bar{Z}')^2}, \text{ or } C_u^2 = \frac{1}{L}$$

where, L is the effective number of looks of the noisy image, and *var*($z'$) and $\bar{Z}'$ are the intensity variance and mean over a homogeneous area of the image, respectively. Clearly, in uniform areas, the value of $C_s$ approaches $C_u$ and $K_s$ nears to zero, leading to the same result as mean filter. At the edges, the value of $C_s$ becomes larger, and $K_s$ nears to unity, resulting in little modification. Kuan filter is considered to be more efficient than Lee filter. The resulting filter for signal dependent noise is the same as Lee filter except for the $K_s$, which is defined as:

$$K_s = \frac{Z' \operatorname{var}(I_s)}{\bar{I}_s^2 \operatorname{var}(Z') + \bar{Z}'^2 \operatorname{var}(I_s) + \operatorname{var}(Z') \operatorname{var}(I_s)}$$

where, $K_s$ provides the noise removed image for further process, whereas this noise removal process can improve the accuracy of entire ACADS.

## 4. IMAGE ENHANCEMENT

One of the simplest and most attractive areas of digital image processing is the Image enhancement. Essentially, the thought behind improvement methods is to bring out detail that is not clear, or just to highlight certain features of interest in an image. A well known case of the upgradation is depicted in Figure 1 in which the contrast of an image is increased and filtered it to evacuate the noise "it looks better." It is predominant to remember that the subjective area of image processing is the image enhancement. The application of enhancement techniques is used for achieving the improvement in the quality of these degraded images.

## 5. ADAPTIVE HISTOGRAM EQUALIZATION METHOD

This method is described as an extension to the traditional Histogram Equalization technique. By using this method, the contrast of images can be enhanced by transforming the values in the intensity image I. It operates on small data regions (tiles), rather than the entire image which is dissimilar to HISTEQ. The contrast of every tile is enhanced such that the histogram of the output region matches the specified histogram approximately. The bilinear interpolation is used for combining the neighboring tiles which helps in eliminating the artificially induced boundaries. The contrast, particularly in homogeneous territories, can be constrained so as to abstain from amplifying the noise which might be available in the image itself. The resultant of the image enhancement process can deliver an enhanced image where it give exact contrast and brightness value of the image.

## 6. MORPHOLOGICAL OPERATIONS BASED OIL SPILL DETECTION

Binary images may contain countless limitations. In some circumstances binary regions established by simple thresholding are secured by noise and textures. Morphology is a wide stretch of image processing operations that modifies the images based on shapes. It is considered to be one of the data processing methods and it is useful in image processing. It contains many applications such as texture analysis, noise elimination, boundary extraction etc.. The goal of the Morphological image processing is eliminating all these defects and maintaining the structure of the image. Morphological operations are assured only on the associated ordering of pixel values, rather than their numerical values, thus they are focused more on binary images, but it can also be utilized to grayscale images such that their light transfer functions are unknown and thus their absolute pixel values are not taken into contemplation. Morphological techniques certify the image with a small template called structuring element. The structuring element can be applied to all possible locations of the input image and produce the same size output. In this technique the output image pixel values depend on similar pixels of the input image with its neighbors. This operation initiates a new binary image in which, if the test is successful, it will have non-zero pixel value of that locale in the input image. There are various structuring elements such as diamond shaped, square shaped, cross shaped etc.

The root of the morphological operation is dilation, erosion, opening, closing expressed in logical AND, OR notation and narrated by set analysis. Among them in this paper only two operations are used dilation and erosion. When erosion removes the pixels at the boundaries of the objects, dilation adds pixels. This removal or adding of pixels based on the structuring element used for processing the image. In mathematical morphology Dilation is one of the basic operators which is applied to binary image, but can also be applied to the grayscale image. Dilation causes the objects to grow in size. The effect of this operation will slowly increase the boundaries

of foreground pixels, so areas grow in size and holes in that region become smaller. Dilation takes two parts as data. The first is the input image to be dilated and the second is the structuring element also known as the kernel. It determines how much the image is to be dilated is only with the help of this structuring element. The mathematical definition of dilation can be as follows:

Suppose A be a set of input image coordinates and B be a set of structuring element coordinates and B$x$ is a translation of B so that its origin is at $x$. Therefore the dilation of A by B is set of all points of $x$ such that intersection of B$x$ with A is not null. In terms of set operations dilation of A by B is defined as:

$$A \oplus B = \{x|(\hat{B})_x \cap A \neq \varnothing\}$$

The output of diluted image is similar to canny edge detection, whereas the edges of the objects inside an image is detected. It look like the regions of the images.

## 7. FILLING THE REGION

Dilation operation makes the boundaries of the object thick, thus for segmenting the object the next step is to fill the holes. The flood fill operation is most commonly known to fill the holes in the given input image. For binary images, it essentially changes the background pixels to foreground pixels until it reaches the object boundaries and for grayscale images it makes the potency level same, i.e. it makes the dark areas enclosed by lighter areas to same intensity levels.

In binary images and grayscale images the boundaries of the objects need to be described by connectivity. In binary images the starting point for filling can also be defined. If we specify holes as an argument, then it is of no need to specify some starting points. In this paper, fill operation is used for binary image with arguments holesand thus it automatically fills the holes of various objects in the image. The output of the filling operation provides the flood fill of dialated image.

## 8. EROSION

Erosion is also one of the basic operators in mathematical morphology. Erosion causes the objects to decrease or become thin in size. Erosion basically dissolves away the boundaries of the foreground which results in areas of those pixels narrower in size and holes of those areas become larger. So, after dilution and filling of the holes of the object in some images the boundaries get mixed up, so as to somewhat separate the boundary erosion, is applied so as to make the boundaries of the objects thinner for better output. Erosion like same dilation takes two parts as data. First one is the input image to be eroded and the second is the structuring element. With the help of this structuring element only it determines how much the image is to be eroded. The mathematical definition of erosion can be as follows:

Suppose A be a set of input image coordinates and B is a set of structuring element coordinates and B$x$ is a translation of B so that its origin is at $x$. Thus, dilation of A by B is set of all points of $x$ such that B$x$ is a subset of A. In terms of set operations, the erosion of A by B is defined as:

$$A \ominus B = \{x|(B)_x \cap A^c \neq \varnothing\}$$

The output of the eroded image shows the accurate shape obtained from the filled image. It provides various filled objects available in the image.

## 9. FEATURE EXTRACTION

Feature extraction is a method of expressing the visual content of images for indexing and retrieval. Feature extraction is used to indicate a piece of information which is pertinent for solving the computational task related

to a certain application. There are two types of texture elements measure. In the first order, texture measures are statistics calculated from an individual pixel and do not consider pixel neighbor relationships. The intensity histogram and intensity elements are first order calculation. In the second order, measures contemplate the relationship between neighbor relationships. The GLCM is a second order texture calculation. In this work, GLCM texture elements are removed from the given input image.

## 10. GLCM

A gray level co-occurrence matrix (GLCM) or co-occurrence distribution (less often co-occurrence matrix or co-occurrence distribution) is a matrix or distribution that is described over an image to be the distribution of co-occurring values at a given offset. A GLCM is a matrix where the number of rows and columns is alike to the number of gray levels, G, in the image The use of statistical elements is therefore one of the earliest methods suggested in the image processing literature. Haralick proposed the use of co-occurrence matrix or gray level co-occurrence matrix. It considers the relationship between two neighboring pixels, the first pixel is known as a reference and the second is known as a neighbor pixel. Given an image I, of size N × N, the co-occurrence, matrix P can be defined as:

$$\mathrm{P}(i,j) = \sum_{x=1}^{\mathrm{N}} \sum_{y=1}^{\mathrm{N}} = 1 \begin{cases} \text{if } \mathrm{I}(x,y) = \mathrm{I} \text{ and } \mathrm{I}(x+\Delta x, y+\Delta y) = i \\ 0, \text{otherwise} \\ \text{the offset } (\Delta x, \Delta y), \text{is spacifying} \end{cases}$$

the distance between the pixels and its neighbours.

### Steps for GLCM

**Step 1:** Read the image content

**Step 2:** Compute the co-occurrence matrix

**Step 3:** Compute the Haralick texture features

**Step 4:** Save acquired information to a DB

The extracted features are :

$$\text{Energy} = \mu = \left(\frac{1}{\mathrm{MN}}\right) \times \sum_{i=1} \sum_{j=1} \mathrm{P}(i,j)$$

$$\text{Contrast} = \sum_{n=0}^{\mathrm{N_g}-1} n^2 \left\{ \sum_{i=0}^{\mathrm{N_g}-1} \sum_{j=0}^{\mathrm{N_g}-1} p_{d,\theta}(i,j) \right\}, \text{ where } n = |i-j|$$

$$\text{Entropy} = \sum_{i=0}^{\mathrm{N_g}-1} \sum_{j=0}^{\mathrm{N_g}-1} p_{d,\theta}(i,j) \log\left(p_{d,\theta}(i,j)\right)$$

$$\text{Correlation} = \sum_{i=0}^{\mathrm{N_g}-1} \sum_{j=0}^{\mathrm{N_g}-1} p_{d,\theta}(i,j) \frac{(i-\mu_x)(j-\mu_y)}{\sigma_x \sigma_y}$$

$$\text{Homogeneity} = \sum_{i,j=0}^{\mathrm{N}-1} \frac{\mathrm{P}_{ij}}{1+(i-j)^2}$$

After extracting the features described above from the image is used for classification. In this paper multi class SVM classifier is used for classification.

## 11. MULTI-CLASS SVM CLASSIFIER

In this paper multi-class SVM classifier is applied to classify the extracted features from the segemented image. It is used to confirm the segemneted object is oil spill from the input image. In general SVM classifier classifies the input dataset in to two different classes as positive or negative (true or false). In order to do classification, a common hyper palne is created in the middle of the data where it divides the entire dataset into two different classes by computing the distances $d_1$ and $d_2$ which is shown in the following Figure 3.

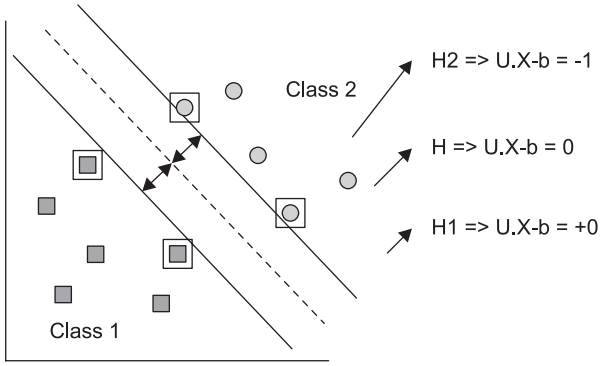


**Figure 3: SVM Classification**

Opposite to Figure 3, instead of Class 1 and Class 2, there are $n$ number of Classes are created according to $H = \{H_1, H_2, ..., H_n\}$.

The entire approach steps of the proposed approach ACADS is experimented and the results are verified.

## 12. EXPERIMENTAL RESULTS AND DISCUSSION

The steps of the proposed approach is implemented and experimented in MATLAB software and the results are obtained in each stage and shown in the following figures.

**Figure 4: Input Image**

**Figure 5: Noise Removed Image**

**Figure 6: Gray Sclaed and Enhanced Image**

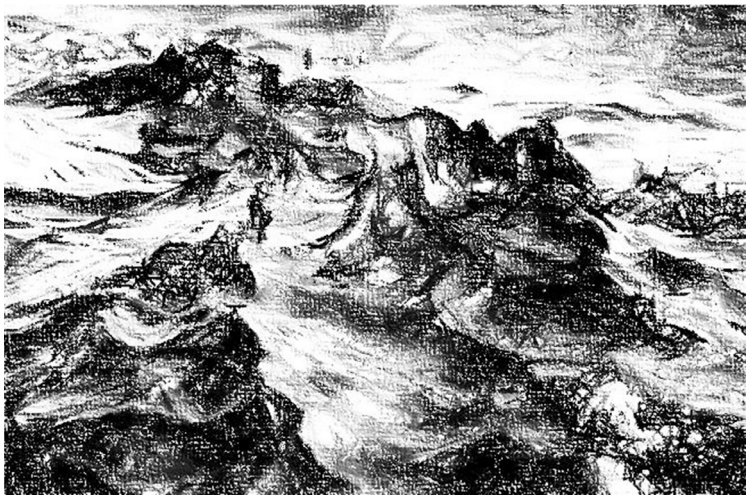

**Figure 7: Binary Image For Binary Operations**

**Figure 8: Detected and Segmented Oil Spill Portion in the SAR Image**

Figure 5 to Figure 8 shows the input image, noise removed image, enhanced image, binary gray scale image, binary image, and oil spill detected image respectively. In order to obtain the accuracy the GLCM features are extracted from the image and feed into Multi-class SVM classifier. According to the feature classification the obtained results is given in Table 1. There are 100 images are taken for experiment and the performance is evaluated.

**Table 1**
**Existing Images versus Classified Images**

| *Images* | *Normal Images* | *OS Images* | *Correctly Classified* | *Wrongly Classified* |
|---|---|---|---|---|
| Database | 50 | 50 | 49 | 1 |

From the above Table 1, it is very clear that the number of normal images available in the database, correctly classified by multi-class SVM and wrongly classified by multi-class SVM. From the number images the TPR, TNR, FPR and FNR is calculated and it is used for computing the sensitivity, specificity and accuracy.

$$\text{TPR} = \frac{\text{Number of OSD correctly obtained}}{\text{Total number of images to be Detected}}$$

$$\text{TNR} = \frac{\text{Number of images correctly identified}}{\text{Total Number of OS images}}$$

$$\text{FPR} = \frac{\text{Number of OSD in-correctly obtained}}{\text{Total Number of images to be Detected}}$$

$$\text{FNR} = \frac{\text{Number of Non-OS images incorrectly identified as OS}}{\text{Total Number of Non-OS}}$$

$$\text{TPR} = \frac{49}{50} = 0.98$$

$$\text{TNR} = \frac{49}{100} = 0.49$$

$$\text{FPR} = \frac{1}{50} = 0.02$$

$$\text{FNR} = \frac{1}{50} = 0.02$$

From the TPR, TNR, FPR and FNR, it concluded and decided that the proposed ACADS approach can provide more accuracy in oil spill detection.

## 13. CONCLUSION

The main objective of this paper is to design and develop an automatic CAD system for identifying, detecting and segmenting oil spill from the SAR images. In order to obtain the oil spill detection accurately the entire ACADS approach is devided into various stages and experimented. In each stage based results are presented and verified by feature extraction and classified. From the obtained results it is concluded that ACADS is suitable for oil spill detection. In future the proposed ACADS is compared with various existing approaches and the performance is evaluated.

## REFERENCES

[1] Lu, J. (2003). Marine oil spill detection, statistics and mapping with ERS SAR imagery in south-east Asia. International Journal of Remote Sensing, 24(15), 3013-3032.

[2] Lu, J., Lim, H., Liew, S.C., Bao, M., & Kwoh, L.K. (1999). Ocean oil pollution mapping with ERS synthetic aperture radar imagery. Proc. IGARSS'99, Vol. 1 (pp. 212-214).

[3] Ivanov, A., He, M. -X., Fang, M. -Q. (2002). Oil spill detection with the RADARSAT SAR in the waters of the Yellow and East China Sea: A case study. Proc. ACRS 2002-23rd Asian Conference on Remote Sensing, November 25-29, 2002, Kathmandu, Nepal.

[4] Espedal, H.A., & Johannessen, O.M. (2000). Detection of oil spills near offshore installations using synthetic aperture radar (SAR). International Journal of Remote Sensing, 21(11), 2141-2144.

[5] Fingas, M. (2001). The basics of oil spill cleanup. Lewis Publishers.

[6] European Space Agency. (1998). Oil pollution monitoring. ESA brochure: ERS and its applications—Marine, BR-128, 1.

[7] Oceanides Web-site. (2004). http://oceanides.jrc.cec.eu.int/prestige.html, accessed 13 August 2004.

[8] Shepherd, I., Bauna, T., Chesworth, J., Kourti, N., Lemoine, G., & Indregard, M. (2004). Use of ENVISAT at JRC for marine monitoring in 2003. JRC Technical Note, (available at: http://pta.jrc.cec.eu.int/entity.

[9] Trieschmann, O., Huns7nger, T., Tufte, L., & Barjenbruch, U. (2003). Data assimilation of an airborne multiple remote sensor system and of satellite images for the North- and Baltic sea. Proceedings of the SPIE 10th int. symposium on remote sensing, conference on remote sensing of the ocean and sea ice 2003Q (pp. 51-60).

[10] Robinson, I. S. (1994). Satellite oceanography. An introduction for oceanographers and remote-sensing scientists. Wiley–Praxis series in remote sensing.

[11] Zhifu, S., Kai, Z., Baojiang, L., & Futao, L. (2002). Oil-spill monitoring using microwave radiometer. Proc. IGARSS'02, Vol. 5 (pp. 2980-2982).

[12] Fingas, M.F., & Brown, C.E. (1997). Review of oil spill remote sensing. Spill Science and Technology Bulletin, 4, 199-208.

[13] Fingas, M. The Basics of Oil Spill Cleanup. CRC Press LLC: USA, 2001.

[14] Li, J. Spill Management for the Toronto AOC: The City of Toronto Study. Report and factsheet prepared for the Great Lakes Sustainability Fund, Burlington, Ontario, Canada. 2002.

[15] "Automatic detection of lung cancer nodules by employing intelligent fuzzy cmeans and support vector machine ", Biomedical Research,August 2016 Impact Factor : 0.226 (SCI, Scopus indexed).

[16] "Cognitive Computational Semantic for high resolution image interpretation using artificial neural network", Biomedical Research, August 2016 Impact Factor : 0.226 (SCI, Scopus indexed).